National Aeronautics and Space Administration

Investigation of Stacking Fault and Antiphase Boundary Segregation in Ni-Based Superalloys Using Density Functional Theory

Brian S. Good and Timothy M. Smith • NASA Glenn Research Center • Cleveland, OH

INTRODUCTION

Ni-based superalloys have a long history of use in jet turbine engines, and efforts to improve their performance in that application are ongoing.

It is known that the precipitation of the Ni3Al γ' phase within the disordered FCC γ phase strengthens the overall material. However, in the high-temperature environment found inside a turbine engine, creep can cause the γ' phase to transform to different, weaker phases, which leads to a deterioration of performance.

In the γ' phase, one mode of creep deformation is the formation of stacking fault ribbons, which consist of intrinsic stacking faults further shearing into antiphase boundaries (APBs). If this shear could be inhibited by the inclusion of certain solute elements near the fault, creep resistance might be improved. In more detail, if an alloying element is found to segregate to, e.g., a stacking fault, but not to, e.g., an antiphase boundary, the glide will likely be more costly energetically, and less likely to occur.

To this end, a density functional investigation was performed on the energetics of segregation of W, Mo and Cr to both a superlattice intrinsic stacking fault (SISF) and an APB.

Earlier DFT studies of similar systems were performed by Rao et al. [1]. This work involved calculating the energetics for Co, Cr, Nb and Ta segregation to stable stacking faults in γ' Ni_3Al. They found that all four solutes are energy-neutral when the solute is located on a Ni, site, and none of the four exhibit segregation when located on an Al site. These calculations were performed using only a single segregating solute atom in a Ni3Al cell with a Superlattice Intrinsic Stacking Fault (SISF) defect.

We are currently performing similar calculations that instead use computational cells that include a variety of solute species that are representative of those in the alloys of interest here. At this time, only preliminary results are available.

DFT Calculations were performed using the Vienna Ab-initio Simulation Package (VASP) plane-wave pseudopotential computer code.[2-4] The calculations incorporated the Projector Augmented Wave (PAW) scheme [5] and used the standard VASP PAW library 5.2 [6]. Atomic relaxation was carried out using a quasi-Newton scheme. A Γ-only k-point grid was used, with further calculations being performed using denser grids. All calculations were spin-polarized.

SISF RESULTS

The first such calculation was performed on an alloy of composition Al 12.5 at% Co 17.2 at% Cr 6.1 at% (W, Mo) 6.1 at% Ni 57.8 at% that is representative of the solute atoms in alloys of interest. These cells are shown in Figure 1.

The segregation energy is defined as the difference between the segregated and unsegregated cells, with a negative energy indicating segregation. It includes energy changes associated with all potentially-segregating species (Co_{Ni}, Cr_{Al} and Mo_{Al} or W_{Al}). In the segregated cell, all potentially-segregating species are confined to the two layers adjacent to the SISF on either side of the defect, so that the segregation energy (Table 1) includes contributions from all those solutes, and quantitative estimates of the segregation of individual species cannot be extracted. It should be noted, however, that according to Rao et al., Co_{Ni} is essentially segregation neutral, and contributes little to the segregation energy in the segregated alloy cell. Cr_{Al}, on the other hand, is energetically unfavorable on the SISF. Because the whole-cell energy is negative for both the Mo- and W-segregated cells, it can be concluded that both Mo and W give large negative contributions to the segregation energy. Additional calculations are under way to provide the single-solute segregation energies.

Additional corroboration of our computational results is provided by observing the atomic relaxation of segregating atoms near an SISF. Shown in Figure 2 are a high-angle annular dark-field scanning transmission electron microscopy (HAADF-STEM)[7] image of a SISF cell, and a graph of relaxations, along with a similar image of our relaxed results from a SISF DFT cell, prepared using the μ-STEM code [8]. It can be seen that the relaxations are qualitatively similar between the experimental and computational results.

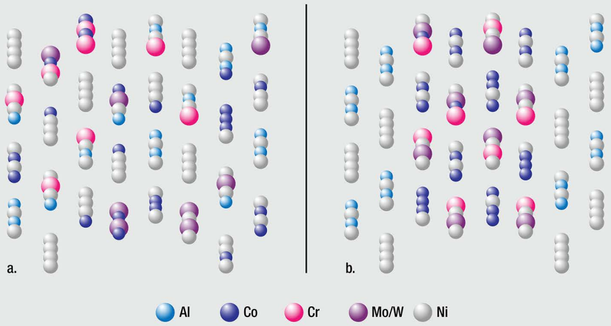

Figure 1. SISF cells with solute atoms placed randomly (a) or in the two layers on either side of the SISF. The SISF is oriented vertically in the center of the cell, between the fourth and fifth vertical atomic planes.

Table 1. Unrelaxed and relaxed whole-cell segregation energies.

Solute	Unrelaxed energy	Relaxed energy
Mo	-3.05eV	-3.39eV
W	-2.97eV	-3.19eV

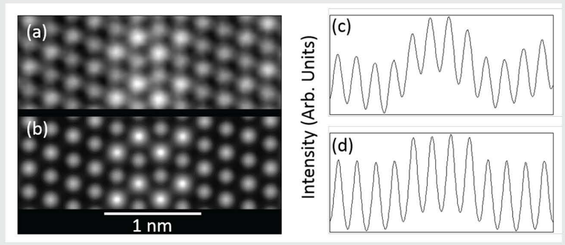

Figure 2: (a) Experimental and (b) simulated HAADF image of a segregated SISF. (c) Experimental and (d) simulated vertically averaged intensity of the images in (a) and (b).

APB RESULTS

At the present time, only calculations performed using isolated solute atoms in Ni3Al cells have been completed. Segregation in cells containing one or two isolated solute atoms were investigated; for segregating cells containing two impurities, both atoms were in the layer adjacent to the defect. Representative APB cells are shown in Figure 3. W, Mo and Cr on Al sites were studied, as well as Cr on Ni sites. Results are shown in Table 2.

It can be seen that, for Al sites, W and Mo do not segregate to the APB boundary, while Cr is essentially neutral in that neither segregation nor randomization is energetically preferred. For Ni sites, Cr does exhibit segregation.

Because Mo and W segregate to the SISF but not the APB, the inclusion of these elements could provide a degree of protection against creep. Researchers in our laboratory have performed preliminary experimental studies that indicate that a significant reduction in creep is possible.

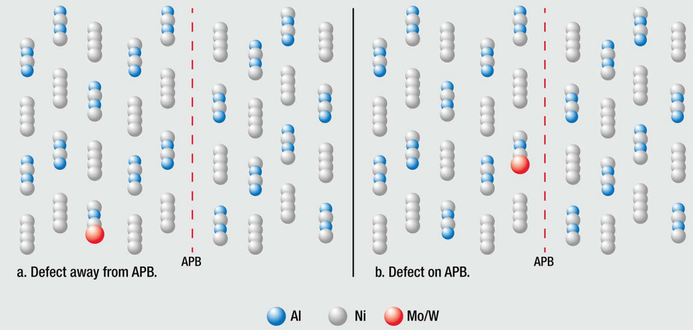

Figure 3. [110] view of the Ni_3Al cell with an APB down its center where the defect atom is placed (a) away from the APB and (b) on the APB.

Table 2. Antiphase boundary segregation energies.

Element	Site Seg.	Energy, eV/atom
W	Al	+0.217
2W	Al	+0.225
Mo	Al	+0.139
2Mo	Al	+0.197
Cr	Al	−6.66e-3
2Cr	Al	+6.15e-3
Cr	Ni	−0.315
2Cr	Ni	−0.136

CONCLUSIONS

Based on DFT calculations, W and Mo exhibit segregation to Al sites on SISF boundaries, while Cr does not. Mo and W do not segregate to Al sites on APBs, while Cr is energetically neutral. Cr does segregate to Ni sites on APBs. Based on these results, and on early experimental work, Mo or W may be effective at reducing creep in NiAl superalloys.

ACKNOWLEDGMENTS

Funding for this study was provided by NASA's Aeronautics Research Mission Directorate (ARMD) – Transformational Tools and Technologies Project and NASA's Advanced Air Transport Technology (AATT) Project Office (ARMD).

REFERENCES

1. Segregation of Alloying Elements to Planar Faults in γ' Ni3Al, Y. Rao, T.M.Smith, M.J.Mills and M. Ghazisaedi, Acta Mater. 148, 15 April 2018, Pages 173-184.
2. G. Kresse and J. Hafner, Phys. Rev. B 47 , 558 (1993); ibid. 49 , 14 251 (1994).
3. G. Kresse and J. Furthmuller, Comput. Mat. Sci. 6 , 15 (1996).
4. G. Kresse and J. Furthmuller, Phys. Rev. B 54 , 11 169 (1996).
5. J.P. Perdew, K. Burke, M Ernzerhof, Generalized Gradient Approximation Made Simple, Phys. Rev. Lett. 77 (1996), 3865-3868.
6. G. Kresse and D. Joubert, Phys. Rev. 59 , 1758 (1999).
7. S.J. Pennycook, Z-CONTRAST TRANSMISSION ELECTRON MICROSCOPY: Direct Atomic Imaging of Materials, Annu. Rev. Mater. Sci. 22 (1992).
8. Modelling the inelastic scattering of fast electrons, L.J. Allen, A.J. D'Alfonso and S.D. Findlay, Ultramicroscopy, Vol. 151, pp. 11-22, (2015).